

Figure S1. The slippage angle distributions for RCR (12-3-12) triblocks with varied  $\pi$ - $\pi$  strength ( $k$ ).

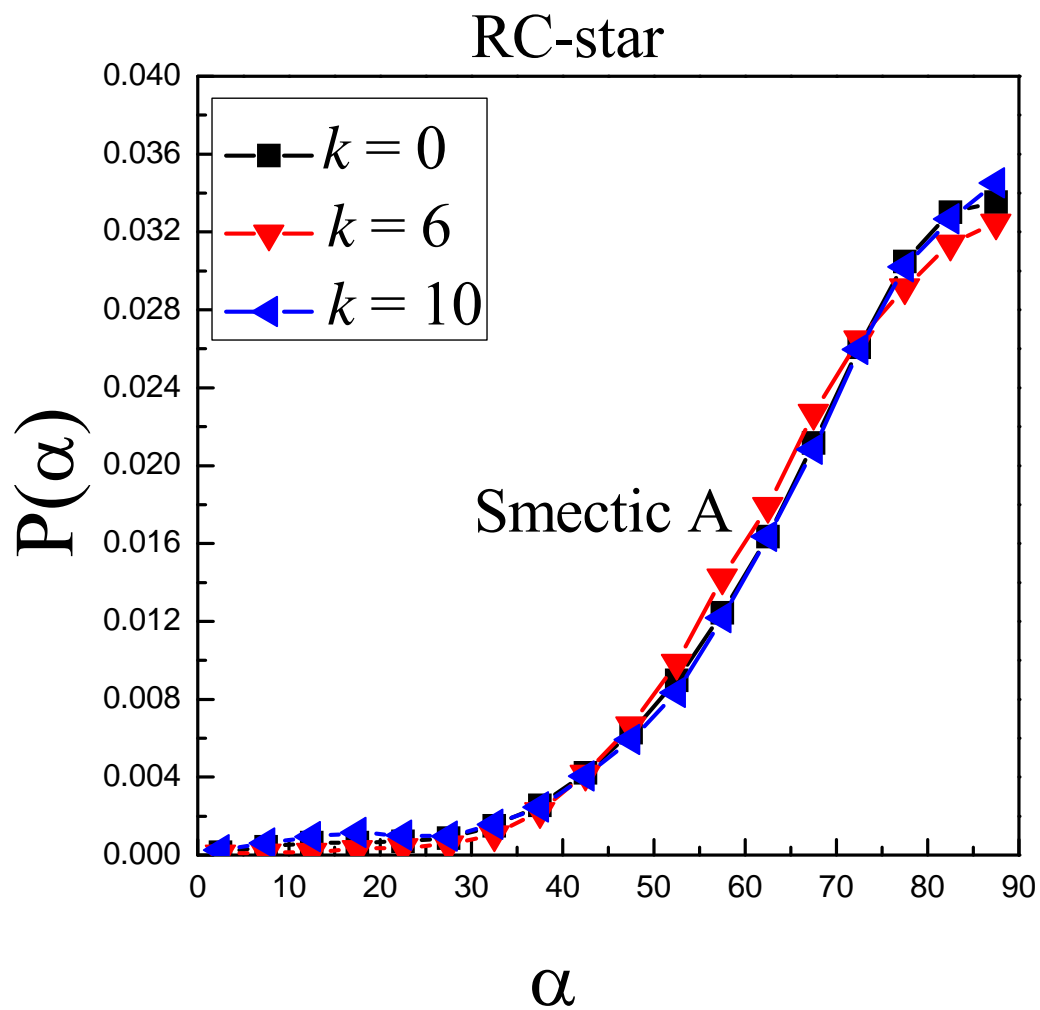


Figure S2. The slippage angle distributions for tri-armed RC-stars with varied  $\pi$ - $\pi$  strength ( $k$ ). The rod and coil lengths are 12 and 4, respectively.

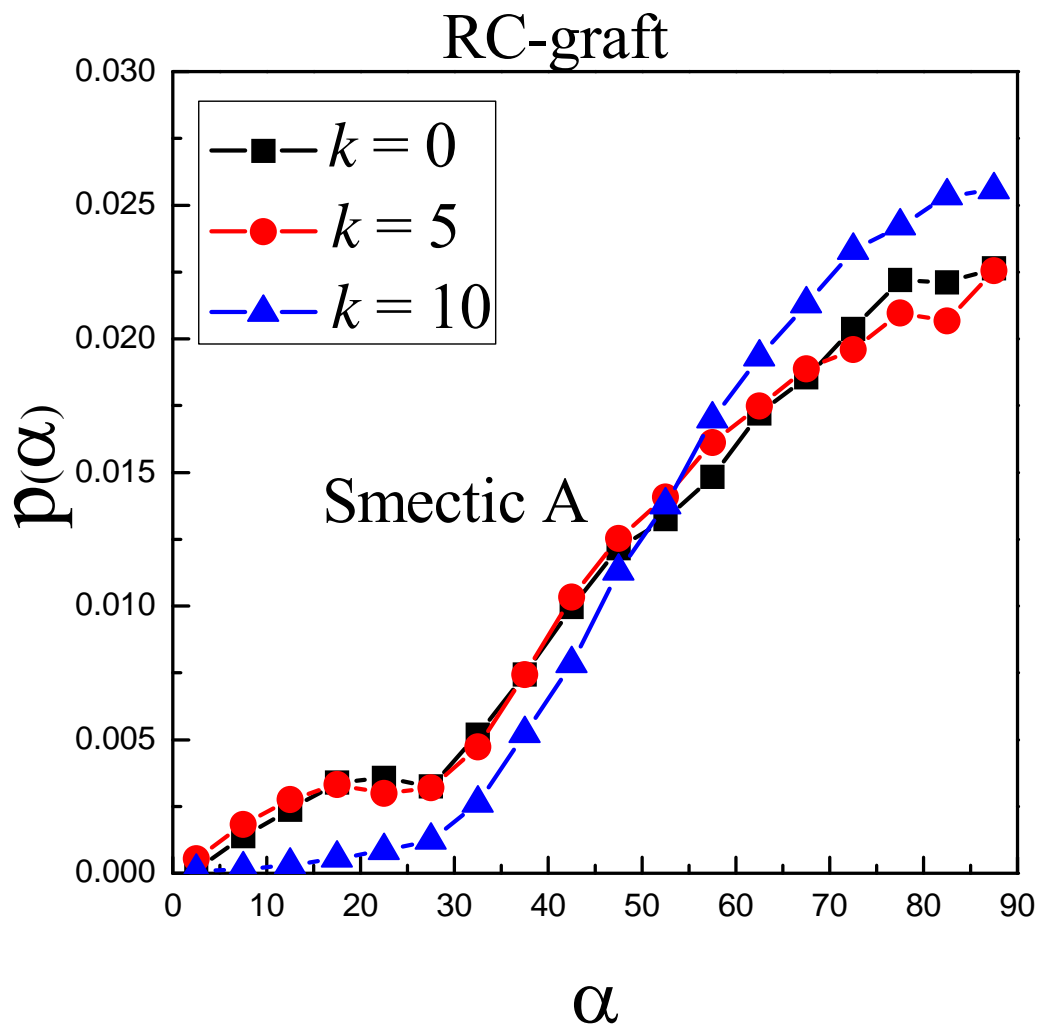


Figure S3. The slippage angle distributions for RC-grafts with varied  $\pi$ - $\pi$  strength( $k$ ). The rod length =9, coil length = 3, and arm number = 4, respectively.

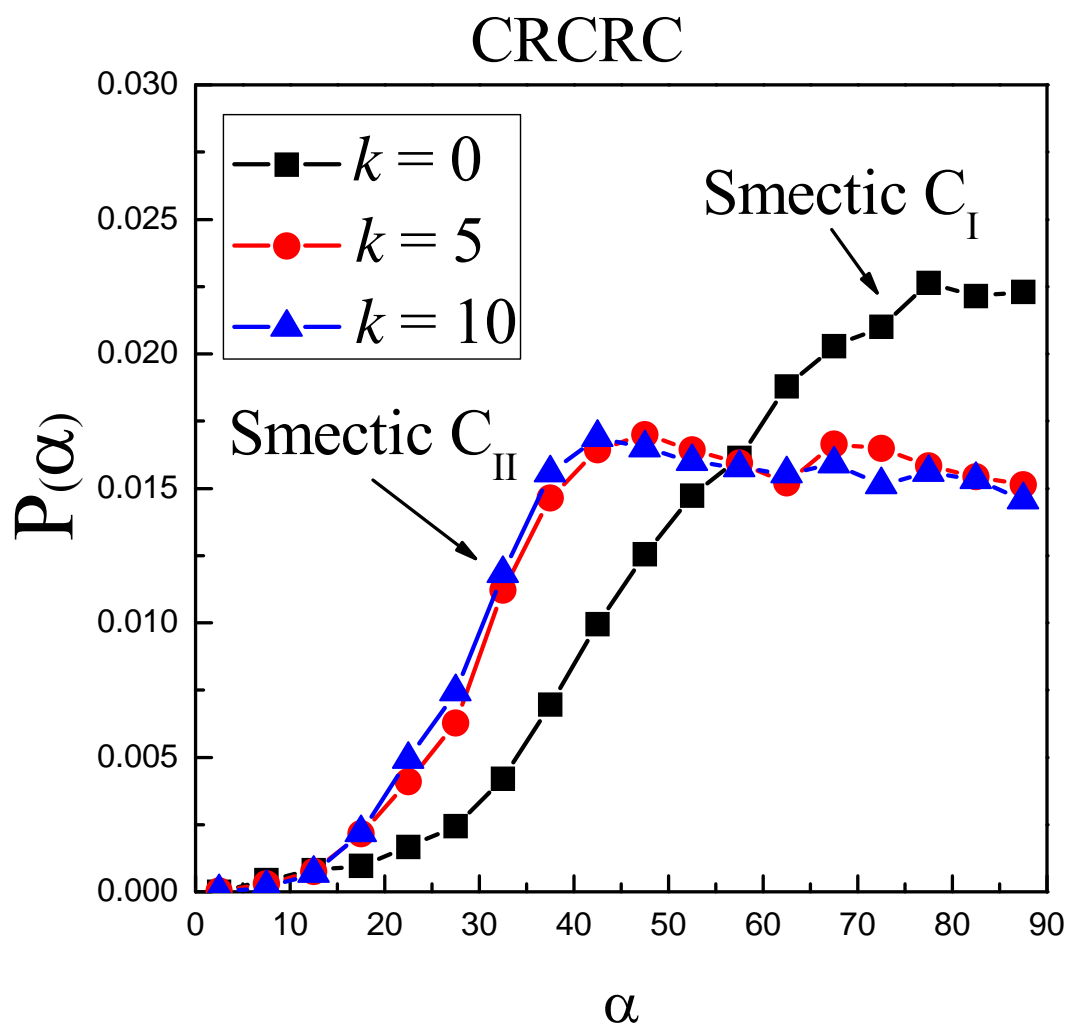


Figure S4. The slippage angle distributions for CRCRC (6-9-6-9-6) pentablocks with varied  $\pi$ - $\pi$  strength ( $k$ ).

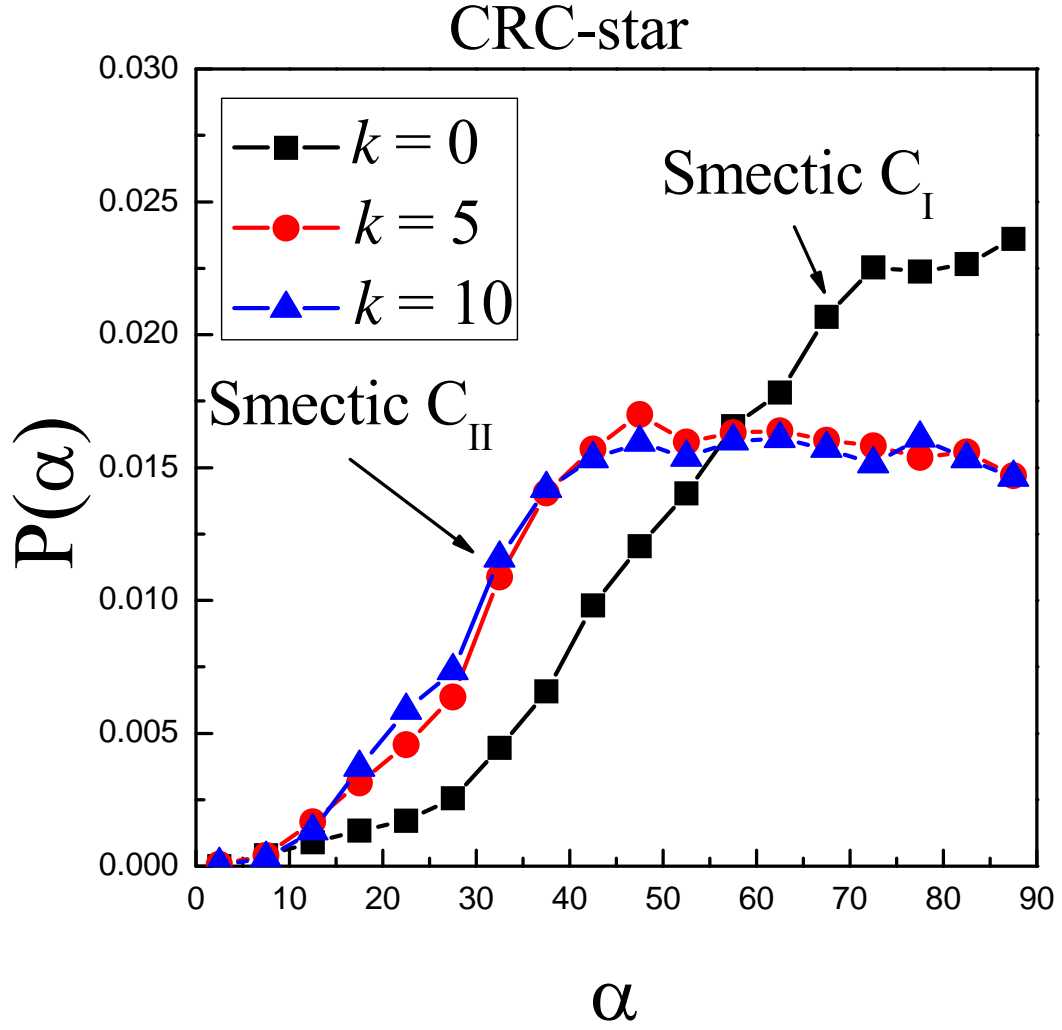


Figure S5. The slippage angle distributions for four-armed CRC-stars with varied  $\pi$ - $\pi$  strength ( $k$ ). The rod and coil lengths are 9 and 6, respectively.

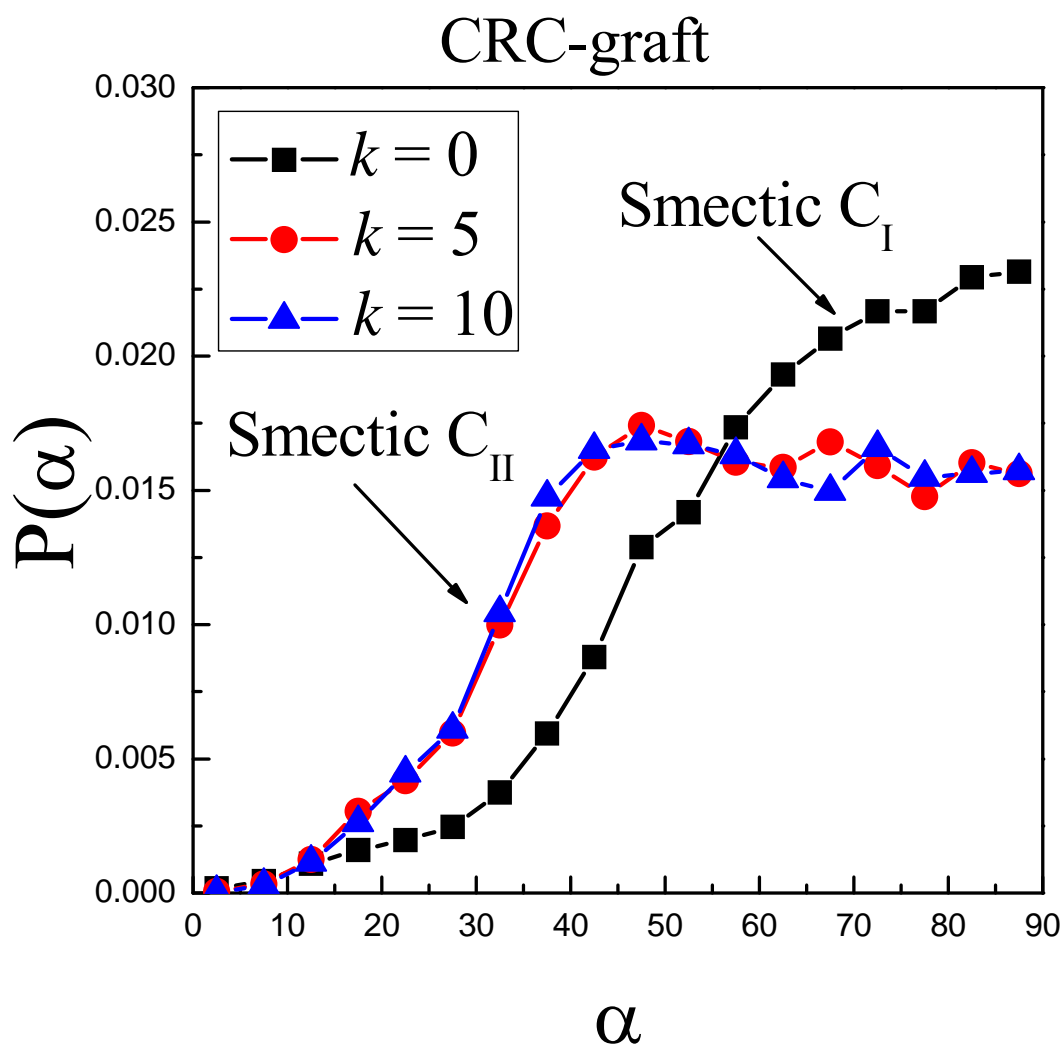


Figure S6. The slippage angle distributions for CRC-grafts with varied  $\pi$ - $\pi$  strength ( $k$ ). The rod length = 9, coil length = 3, and arm number = 6, respectively.

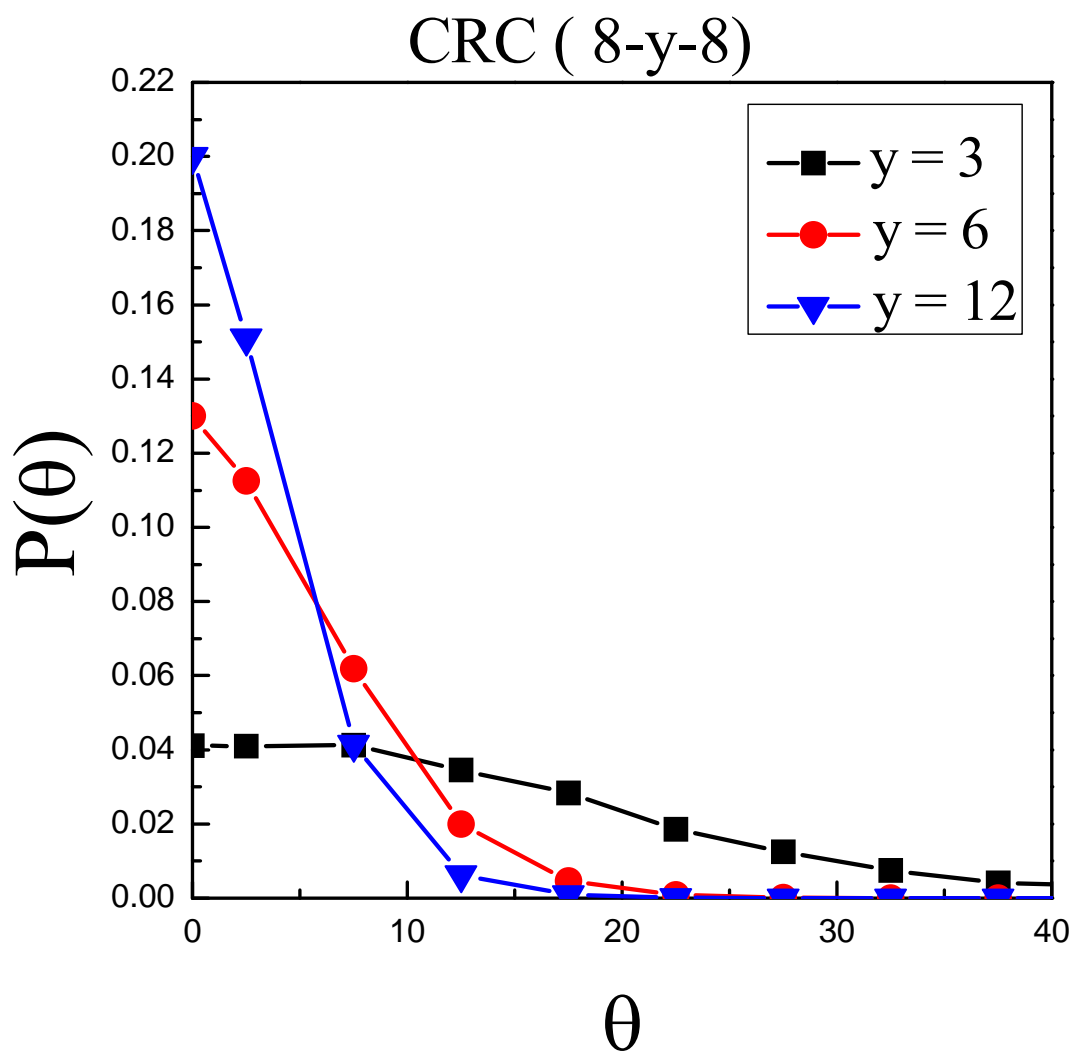


Figure S7. The included angle distributions for CRC (8-y-8) triblocks with varied rod length ( $y$ ).

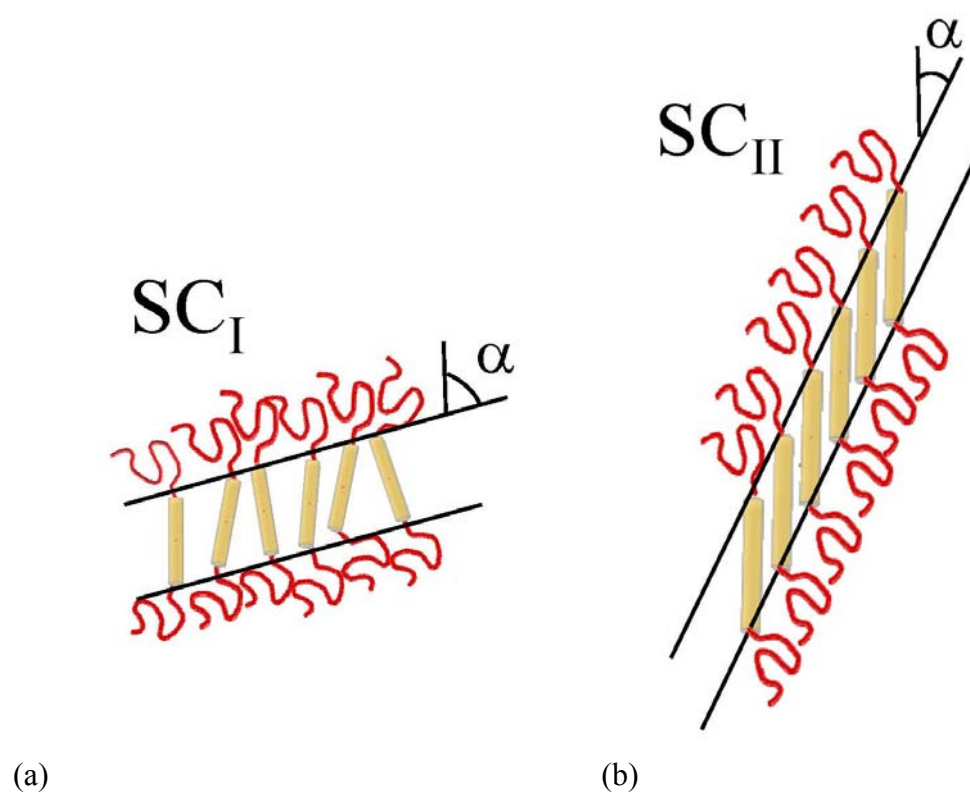


Figure S8. The schematic representations of the  $SC_I$  phase and  $SC_{II}$  phase. (a) Less parallel alignment leads to more space for coil. Small slippage is required and  $SC_I$  phase forms. (b) More parallel alignment results in less space for coil. Large slippage is required and  $SC_{II}$  phase occurs.